Supporting Information

Photoluminescent Enzymatic Sensor Based on Nanoporous Anodic Alumina

Abel Santos, Gerard Macías, Josep Ferré-Borrull, Josep Pallarès

and

Lluís F. Marsal*

Departament d'Enginyeria Electrònica, Elèctrica i Automàtica

Universitat Rovira i Virgili

Avda Països Catalans 26 - 43007 Tarragona (Spain)

1S. Fabrication conditions of nanoporous anodic alumina

The NAA samples were fabricated by the two-step anodization process and the fabrication conditions of these are summarized in **Table 1S**.[12]

Label	*Acid*	V_{an} (V)	t_{an} – 1st step (h)	t_{an} – 2nd step (min)	t_{pw} (min)
Bio (1)				90	0
Bio (2)				“	2.5
Bio (3)				“	5
Bio (4)				105	0
Bio (5)	$H_2C_2O_4$ 0.3 M	40	20	„	2.5
Bio (6)				“	5
Bio (7)				120	0
Bio (8)				“	2.5
Bio (9)				„	5

Table 1S. Fabrication conditions of each NAA sample (V_{an} = Anodization voltage).

2S. Geometric characteristics of nanoporous anodic alumina

The geometric characteristics of the resulting NAA samples were estimated by SEM image analysis. The results are summarized in **Table 2S**.

Label	L_p (μm)	d_p (nm)	d_{int} (nm)
Bio (1)	5.3 ± 0.1	30 ± 2	103 ± 4
Bio (2)	"	34 ± 2	
Bio (3)	"	39 ± 2	
Bio (4)	6.2 ± 0.1	30 ± 2	
Bio (5)	„	34 ± 2	
Bio (6)	"	39 ± 2	
Bio (7)	7.1 ± 0.1	30 ± 2	
Bio (8)	"	34 ± 2	
Bio (9)	„	39 ± 2	

Table 2S. Geometric characteristics of each NAA sample (d_{int} = Interpore distance).

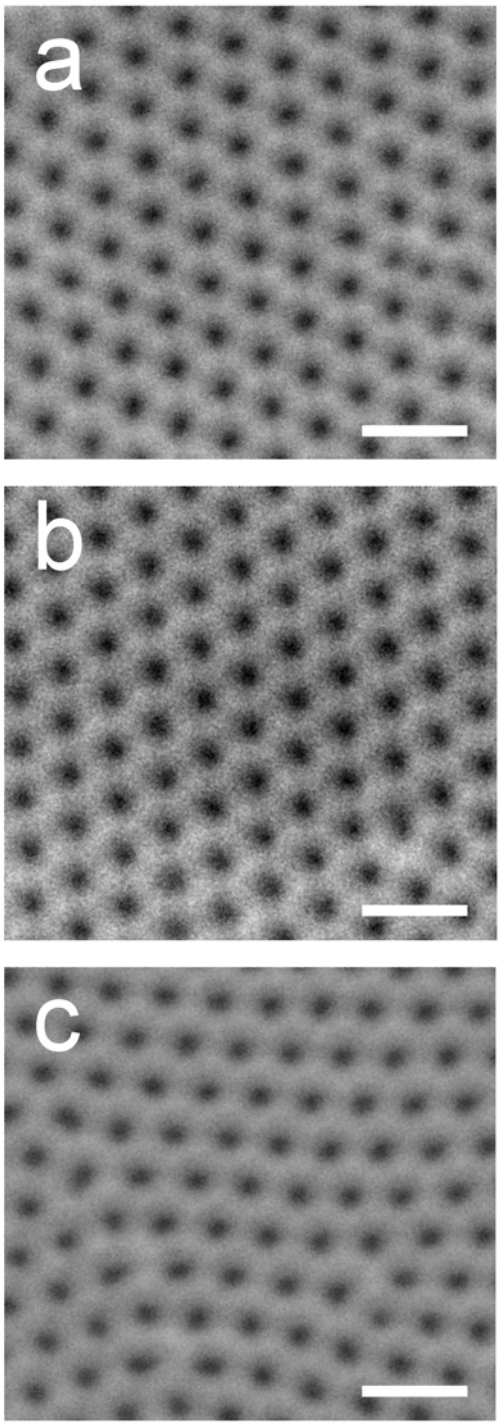

Figure 1S. Set of top view SEM images of several NAA samples (scale bar = 200 nm).

a) Bio (1) d_p = 30 ± 2 nm. b) Bio (2) d_p = 34 ± 2 nm. c) Bio (3) d_p = 39 ± 2 nm.

3S. Change in the effective optical thickness increment

The change in the effective optical thickness increment was estimated from the PL spectra by calculating the slope of the linear fitting *m versus* λ^{-1}. The results are summarized in **Table 3S**.

	ΔOT_{eff} (%) – STAGE		
Label	APTES Functionalization	GTA Activation	Trypsin Immobilization
Bio (1)	0.6 ± 0.2	1.2 ± 0.2	1.8 ± 0.3
Bio (2)	0.8 ± 0.3	0.9 ± 0.3	3.3 ± 0.3
Bio (3)	0.4 ± 0.2	0.3 ± 0.2	2.6 ± 0.3
Bio (4)	0.6 ± 0.3	0.7 ± 0.3	1.9 ± 0.3
Bio (5)	0.8 ± 0.3	0.7 ± 0.3	2.4 ± 0.3
Bio (6)	0.7 ± 0.3	1.0 ± 0.3	1.8 ± 0.3
Bio (7)	0.6 ± 0.3	0.8 ± 0.2	1.7 ± 0.2
Bio (8)	0.6 ± 0.3	1.0 ± 0.3	1.4 ± 0.3
Bio (9)	0.5 ± 0.2	0.6 ± 0.2	2.6 ± 0.3

Table 3S. Change in the effective optical thickness increment after each fabrication stage.

4S. Fourier transform infrared analysis

Each stage of the fabrication process was studied by Fourier transform infrared (FTIR). To this end, the remaining aluminum substrate was removed from the backside of a NAA proof by wet chemical etching in a saturated solution of hydrochloric acid and cupric chloride (HCl / $CuCl_2$). The results are shown in **Figure 2S**. The FTIR spectrum of the as-produced NAA sample was used as a background. The peaks located around 3300, 1600 and 1000 cm^{-1} are related to primary and secondary amines, which increase after each fabrication stage (i.e. APTES functionalization, GTA activation and Trypsin immobilization).

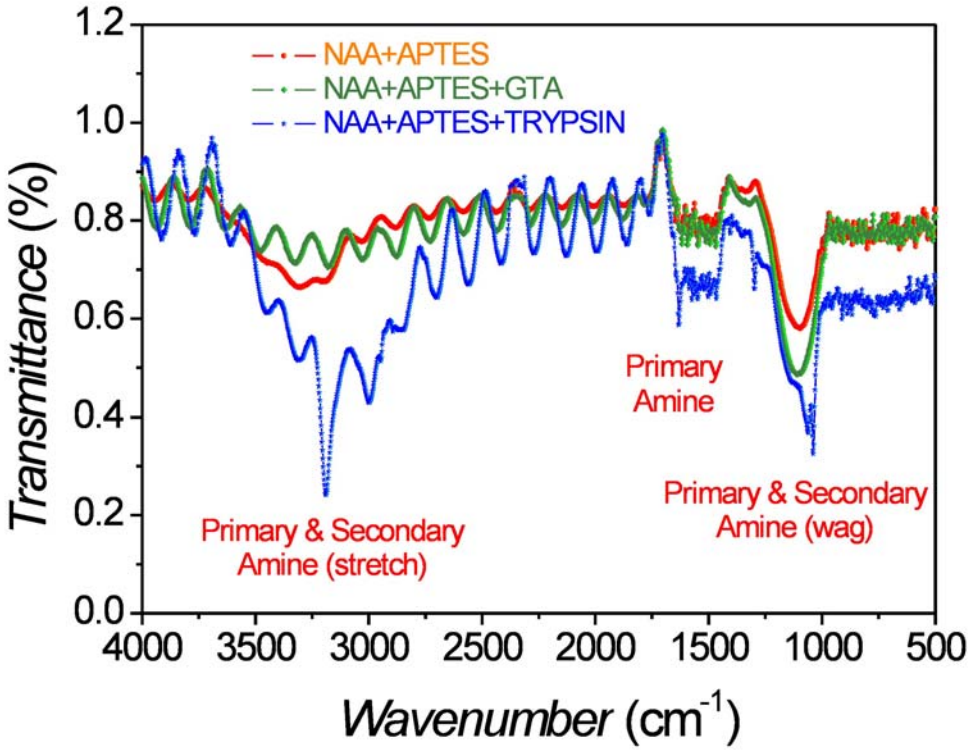

Figure 2S. FTIR transmittance spectra of a NAA sample after each stage of the fabrication process (background = as-produced NAA).